



# A comparison of four methods for extracting Land Surface Emissivity and Temperature in the Thermal Infrared Hyperspectral Data

Faezeh Soleimani Vostikolaee, Mehdi Akhoondzadeh\*

School of Surveying and Geospatial Engineering, College of Engineering, University of Tehran, Tehran, Iran

## Article history:

Received: 12 August 2017, Received in revised form: 25 April 2018, Accepted: 10 May 2018

## ABSTRACT

Land Surface Temperature (LST) and Land Surface Emissivity (LSE) are two important physical properties of Earth's surface. LST retrieval plays a valuable role in environmental studies. Therefore, in order to estimate LST accurately, it is necessary to obtain LSEs. The HyTES (Hyperspectral Thermal Emission Spectrometer) instrument has 256 spectral bands covering the thermal infrared (TIR) spectral range. Due to a large number of narrow bandwidths of HyTES, this sensor can produce the accurate LST and LSEs. The main goal of this paper is to evaluate the accuracy of LSE and LST retrieval methods from HyTES data and to improve the accuracy of the Normalization (NOR) method. For this purpose, four different methods have been considered to retrieve LSE: (i) the Reference Channel method (REF), (ii) the Emissivity Normalization method, (iii) the Alpha emissivity method (ALPHA) and (iv) a method to improve the NOR algorithm. The first three methods have been widely used with thermal multispectral data in other researches. These methods were used with HyTES hyperspectral data in this paper; the fourth is a new method that improved the accuracy of the NOR method. The results of quality assessment show that the emissivity RMSEs of the REF, NOR, ALPHA methods and the new proposed method are 0.021, 0.815, 0.034 and 0.0201, respectively. Also, LST RMSEs of the REF and NOR methods are less than 1.5 K.

## KEYWORDS

LSE  
HyTES  
REF  
ALPHA

## 1. Introduction

Accurate retrieval of land surface temperature (LST) and land surface emissivity (LSE) are of great importance for many applications, such as global change studies, heat balance studies, climate research, and short or medium range forecasts (Wang et al., 2013; Dash et al., 2002; Singh & Bhatia, 2007; Tang et al., 2013). In addition, LSE, as an intrinsic property of natural materials, is often regarded as an indicator of material composition, although it varies with the viewing angle and the surface roughness (Li et al., 2013; Sobrino et al., 2001; Sobrino et al., 2005). Emissivity depends on many factors such as surface roughness, wavelength, the physical and chemical structure of the object and the viewing angle (Brandt et al., 2008; Bagavathiappan et al., 2013; Marinetti & Cesaratto, 2012; Nunak et al., 2015). In general, the emissivity of a real surface tends to emit in a

given wavelength or in a given direction, or in integrated averages over a wavelength and direction (Nunak et al., 2015).

Compared to traditional measurement instruments, satellites can monitor those parameters around the world with a higher spatial and temporal resolution and can provide more opportunities to promote the development of related disciplines (Brandt et al., 2008; Marinetti & Cesaratto, 2012; Tang et al., 2013). Although remote sensing remains the best way to obtain the emissivity over a large area, retrieving LSE from multispectral data cannot produce an accurate emissivity, due to the complicated land surfaces and relatively inadequate measurement information (Nunak et al., 2015). Undoubtedly, hyperspectral data is superior in comparison to the multispectral data in extracting the land surface parameters because the radiance measured during the

\* Corresponding author

E-mail addresses: faezeh.soleimani@ut.ac.ir (F. Soleimani); makhonz@ut.ac.ir (M. Akhoondzadeh)

DOI: 10.22059/eoge.2018.239666.1011

daytime in the mid-infrared (MIR) spectrum contains both the surface emitted thermal radiance and the reflected solar radiance, which are equal in magnitude. The large number of narrow bandwidth of hyperspectral sensors makes them useful tools for exploiting the information contained in discrete absorption features of both atmospheric constituents and the land surface. In addition, they can improve the vertical resolution of atmospheric soundings so the objects even with close spectra can be distinguished from each other and their emissivity can be calculated (Gillespie et al., 1999; Borel, 2003; Brandt et al., 2008). Thus, the thermal hyperspectral data will play a valuable role in researches conducted in the remote sensing community.

There have already been some studies investigating the retrieval of LSE and LST using hyperspectral data. In 1997, Borel proposed an iterative method to separate LST and LSE from the hyper-TIR data for which the atmospheric influence had been well corrected (Borel, 1998). This method is based on (1) in-scene atmospheric transmission estimation (Young et al., 2002), (2) matching of the transmission to a database and (3) retrieving a spectrally smooth emissivity by an iterative method is used on hyperspectral data (Borel 2003, 1998). In 2008, Borel improved the automatic retrieval of temperature and emissivity using the spectral smoothness (ARTEMISS) through a look-up table to determine the best-fitting atmosphere that results in the smallest residual to the In-Scene Atmospheric Compensation (ISAC) estimated transmission (Borel,2008). Another technique to retrieve surface parameters is the neural network (NN) technique. Artificial neural network (ANN) has already been used to retrieve atmospheric profiles as well as LST from hyper-TIR data (Aires et al., 2002; Wang et al., 2010; Wang et al., 2013). Sobrino et al obtained LST from airborne hyperspectral scanner thermal band in three different methods (Sobrino et al., 2006): the single-channel method; (ii) the split-window method (Labbi & Mokhnache, 2015); and (iii) the temperature emissivity separation (TES) method. The results of this study showed that the single-channel and split-window methods provided similar results and the TES method slightly improved the results.

All of the LSE retrieval methods can be categorized into (1) (semi-) empirical or theoretical methods, (2) multi-channel temperature emissivity separation method (Zhong et al., 2016), and (3) physically based methods (Li et al., 2013). The empirical methods that estimate LSE involve classification-based emissivity method and NDVI-based emissivity method. In the classification method, each pixel is placed in one of the emissivity classes after a conventional classification of the land cover, the seasonal, dynamic parameters and based on the reference tables (Chen et al., 2016; Sun & Pinker 2003; Peres & DaCamara, 2005; Zhao et al., 2014). In the NDVI method, based on the relationship between the land surface emissivity and the logarithm of the NDVI, LSE can be found (Rozenstein et al., 2014; Valor &

Caselles, 1996; Sobrino & Raissouni, 2000). The TES method that was proposed by (Gillespie et al., 1999) provides surface emissivity jointly with the temperature (Oltra-Carrió et al., 2014; Gillespie et al., 1998; Hu et al., 2015; Jacob et al., 2017). In 2011, the TES method was improved using a linear spectral emissivity constraint (Wang et al., 2011). Finally, the physically based methods that proposed by (Li et al., 1999) include Channel Radiance, Reference channel, Normalization emissivity, Temperature-Independent Spectral Indices, Emissivity Renormalization, and the Alpha emissivity methods.

To benefit from the hyper-TIR data, this work is devoted to retrieving LST and LSE from HyTES hyperspectral data. The main goal of this paper is to evaluate the accuracy of LSE and LST retrieval methods from HyTES data as well as to improve the accuracy of the NOR method. For this purpose, four different methods have been considered to retrieve LSE: (i) the Reference Channel method (REF), (ii) the Emissivity Normalization method, (iii) the Alpha emissivity method (ALPHA) and (iv) improving the NOR method. The first three methods have been widely used with thermal multispectral data in other researches. These methods were used with HyTES hyperspectral data in this paper. The fourth approach is a new method that improved the accuracy of the NOR method. In addition, LST was derived by these methods in this study. The advantage of these methods is that the emissivity information can be derived for all thermal hyperspectral bands.

This article is organized as follow. The description of a HyTES sensor is presented in section 1.1. In section 1.2 - 1.4, the physical-based methods are recalled. The NOR improving method is given in section 2. The HyTES preprocessing steps are described in section 3. In next section, the proposed methods are applied to HyTES data. Also, the analysis of different methods is given to assist the selection of methods in various circumstances are drawn in section 4. Finally, the conclusion of these methods is given in section 5.

### 1.1 HyTES Sensor

HyTES (Hyperspectral Thermal Emission Spectrometer) is an airborne imaging spectrometer with 256 spectral channels between 7.5 and 12 micrometers in the thermal infrared part of the electromagnetic spectrum and 512 cross-track pixels. HyTES is being developed to support the Hyperspectral Infrared Imager (HypIRI) mission. HypIRI includes two instruments mounted on a satellite in Low Earth Orbit. There is an imaging spectrometer measuring from the visible to shortwave infrared (VSWIR) and a multispectral thermal infrared (TIR) imager. The VSWIR and TIR instruments will both have a spatial resolution of 60 m at nadir. HyTES will provide the HypIRI Group data at much higher spatial and spectral resolutions to help determine the optimum band positions for the HypIRI-

TIR instrument as well as to provide the precursor datasets for Earth Science research in TIR. HyTES completed its first flights in July 2012 (Rivera, 2012).

**1.2 Reference Channel Method**

The Reference Channel method (REF) was developed by (Kahle et al., 1980). The method assumes that the emissivity in one channel has a constant value for all pixels, that is  $\epsilon_r = k$ . Assuming that the emissivity in the reference channel and the atmospheric parameters ( $L_u$ ,  $\tau_r$  and  $L_d$ .) are known, LST can be derived from the measured radiance for each pixel in Eq (1).

$$T_s = \frac{C_2}{\lambda_r \text{Ln} \left[ \frac{\epsilon_r C_1}{L_r \lambda_r^5 \pi} + 1 \right]} \quad (1)$$

where  $L_r$  is the measured radiance at the sensor,  $C_1=1.191 \times 10^8$  (W  $\mu\text{m}^2$  sr<sup>-1</sup> m<sup>-2</sup>),  $C_2=1.439 \times 10^4$   $\mu\text{m}$  K and  $\lambda_r$  is the wavelength of the reference channel r.

The computed LST is then used to calculate the emissivity values for the remaining channels.

$$\epsilon_j = \frac{\frac{L_j - L_u}{\tau_j} - L_d}{B_i(T_s) - L_d} \quad (2)$$

where  $\epsilon_j$  is the emissivity in band i.  $L_u$ ,  $\tau_r$  and  $L_d$  are the atmospheric up-welling radiance, the transmittance and atmospheric dawn-welling radiance parameters, respectively. Finally, by using the emissivity, the actual temperature is obtained from Planck's law using Eq. (1).

**1.3 Alpha Emissivity Method**

The alpha derived emissivity method was developed by (Kealy 1990) based on Wien's approximation of the Planck function:

$$L_j = \frac{C_1}{\lambda_j^5 [\exp(\frac{C_2}{\lambda_j T})]} \quad (3)$$

where  $L_j$  is the blackbody radiance,  $C_1$  and  $C_2$  are Planck's constants, T is the temperature of the blackbody and  $\lambda_j$  is the wavelength of channel j ( $\mu\text{m}$ ). Wien's approximation neglects the - 1 term, making it possible to linearize the approximation with logarithms (Kealy and Hook 1993). The Alpha emissivity method can be broken down into the following steps:

- a) Taking natural logs of the radiance ( $L_j$ ) using Wien's approximation.
- b) Subtracting natural logarithms of one channel from its mean for N channels in order to eliminate the surface temperature T.

Finally,  $\alpha$  for channel j can be defined using the below equations:

$$\alpha_j = \lambda_j \text{Ln}(\epsilon_j) - \frac{1}{N} \sum_{k=1}^N \lambda_k \text{Ln}(\epsilon_k) \quad (4)$$

Kealy (1990) showed that:

$$\alpha_j = \lambda_j \text{Ln}(L_j) - \frac{1}{N} \sum_{k=1}^N \lambda_k \text{Ln}(L_k) + K_j \quad (5)$$

where  $K_j$  is a constant value that depends on the characteristics of the channel. So  $\alpha_j$  can be obtained from the measured radiance ( $L_j$ ).

Estimating the emissivity ( $\epsilon_j$ ) from Eq. (4) is not solvable, since the mean of emissivity values is not known. One of the ways to solve this problem is to use the REF method.

c) The relative emissivity in Channel j with respect to reference channel r can be easily obtained by Eq (6) (Li et al., 1999).

$$\frac{\epsilon_j}{\epsilon_r} = (\exp(\alpha_j - \alpha_r))^{\frac{1}{\lambda_j}} \quad (6)$$

where  $\epsilon_r$  is the emissivity in reference band r,  $\alpha_r$  is the alpha emissivity in reference band r and  $\alpha_j$  is the alpha emissivity in band j.

In addition, the land surface temperature is obtained from Planck's law in Eq. (1) using these emissivity values.

**1.4 Emissivity Normalization Method**

This approach is similar to the reference channel method and was described in (Gillespie, 1985). It assumes a constant emissivity value in all N channels for a given pixel, which enables N temperatures to be calculated for each pixel using Eq. (1) from their radiance, provided that the atmospheric parameters ( $L_u$ ,  $\tau_r$  and  $L_d$ ) are known. The maximum of those N temperatures is considered as LST and is used to derive the emissivity values for other channels using Eq. (2). If the maximum of temperatures for a given pixel occurs in Channel k, this means that the emissivity in Channel k is maximum for this pixel (Li et al., 1999). Finally, by using the computed emissivity, the actual temperature is obtained from the Planck function using Eq. (1).

The advantages of the NOR method compared to the REF method are that in the NOR method, the emissivity values are not equal for all pixels and this method is simple in application.

**2. Improve NOR Method**

This approach is similar to the Emissivity Normalization method. In this method, same as the NOR procedure, assuming that the atmospheric parameters ( $L_u$ ,  $\tau_r$  and  $L_d$ ) are known, a constant emissivity value ( $\epsilon_0 = 0.99$ ) is considered in N channels for a given pixel, which enables N temperatures to be calculated for each pixel using Eq. (1). In order to calculate the land surface emissivity from the measured radiance, it is necessary to smooth the calculated temperatures. The calculated temperatures in Eq. (1) are related to the blackbody or near the blackbody surfaces. If

the maximum record of N temperature is chosen for each pixel (same as the NOR method), the obtained LST will only belong to the areas with a blackbody surface. Therefore, for non-blackbody surfaces, the NOR method acts like as a blackbody area. Moreover, the land surface emissivity that is obtained from this temperature is related to the blackbody surfaces, so these LSEs are higher than their real values. To solve this problem, the mean value of those N temperatures was considered as LST, and was used to derive the emissivity for other channels using Eq. (2). Using this method, the calculated temperature and emissivity values are not related only to the blackbody surfaces. Finally, LST is derived from Planck's law in Eq. (1) using these emissivity values.

### 3. Data Preprocessing

In this study, a HyTES image was used, which was taken from the Aliso Canyon in Orange County of California on 26 January 2016. In the preprocessing stage, the noisy and water vapor absorption bands of the HyTES imagery were removed and its optimal bands were selected. For choosing the optimal bands of this image, the NEDT (Noise Equivalent Delta Temperature) and header file of the related HyTES sensor were used. According to the header file of HyTES image, the spectral bands located in the range of 7.5-8  $\mu\text{m}$  were affected by the vapor absorption properties, so the spectral bands were removed in this range (28 bands). In Figure 1, the NEDT of the HyTES sensor is shown. As shown in this Figure, the noise has increased dramatically in the range of 11.5-12  $\mu\text{m}$ , so the spectral bands in this range, which include 25 spectral bands, were eliminated. Finally, 202 optimal bands in the spectral range of 8-11.5  $\mu\text{m}$  were selected.

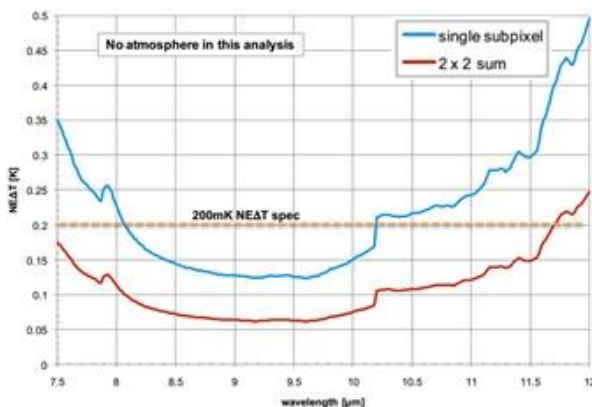


Figure 1. Noise Equivalent Delta Temperature (NEDT) for HyTES

### 4. Discussion

In this section, the Reference Channel method was applied to retrieve the emissivity from HyTES image. The main idea of the REF method is that emissivity in one channel has a constant value for all pixels. Using this assumption, the emissivity is obtained. Moreover, LST is calculated from the inverse of the Planck function.

In the next step, the Alpha Emissivity method was used to retrieve LSE. This method is based on taking the natural logs of the radiance using Wien's approximation and eliminating the land surface temperature when considering the equation for one channel. The emissivity results of the Alpha method are almost the same as the REF method. In the following, the Normalized Emissivity Method was used to retrieve LST and LSE from HyTES data. An initial emissivity value of 0.99 was chosen and the maximum value of N calculated temperatures was considered as LST. Using this temperature, the final emissivity values were recalculated. Finally, the land surface temperature was calculated from the inverse of the Planck function. In order to improve the accuracy of the NOR method, the new method was suggested (section 2), which smoothed the emissivity. In the NOR method, the calculated temperature (Eq. (1)) is related to the blackbody surfaces, so the final emissivity is also related to the blackbody surfaces. In this method, using the mean value of N temperatures, the calculated emissivity is smoothed.

For quality assessment, LSEs that were retrieved from REF, ALPHA, NOR and the newly proposed methods were compared with the emissivity product of the HyTES sensor. In addition, LSTs that were calculated from these methods were compared with the LST product of the HyTES sensor. Statistical analysis on the errors of calculated values of LSE for these methods, including the standard deviation of the error (SDE) and the root-mean-square error (RMSE) are presented in Table 1. The results of statistical analysis on the errors of calculated values of LST in these methods are shown in Table 2. As the results show, these methods are proposed for calculating LST and LSE in HyTES images. The RMSEs for LST obtained REF, ALPHA, NOR and the new proposed methods are 1.41, 2.06, 1.84 and 1.6, respectively. In addition, RMSEs for land surface emissivity values that were obtained from REF, ALPHA, NOR and the new proposed methods are 0.021, 0.815, 0.034 and 0.0201, respectively.

For more analysis, a graph was used to compare the results. In Figure 2 the results of the obtained LSEs from REF, ALPHA, NOR and the new method are presented. Also, in Figure 3 the results of comparison between LST that was obtained from REF, ALPHA, NOR and the new method with the HyTES LST product are shown.

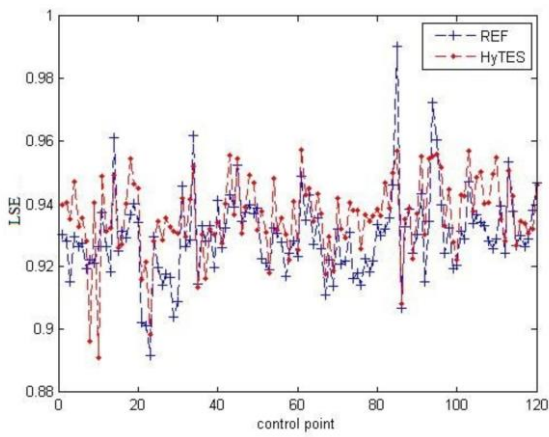
Finally, in Figure 4 the LST maps that were obtained from REF, ALPHA, NOR and the new method are presented. For a better visual comparison, the same area was pointed in each LST map in Figure 4. In the specified areas, the differences between the HyTES LST and LST derived from NOR, REF, ALPHA and the new method are obvious.

Table 1. The results of the evaluation of proposed algorithms

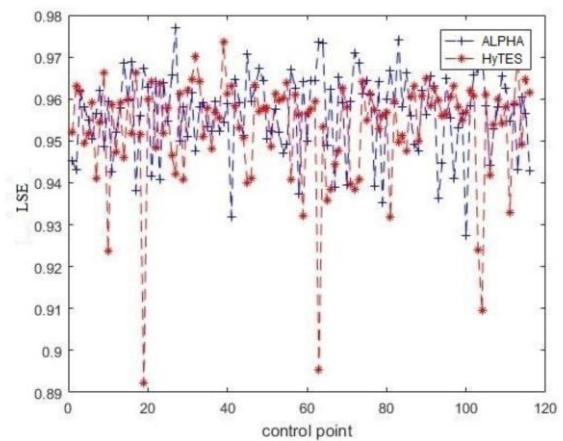
	REF		ALPHA		NOR		New Method	
	RMSE	SDE	RMSE	SDE	RMSE	SDE	RMSE	SDE
<b>LSE</b>	0.021	0.0001	0.815	0.0118	0.034	0.004	0.0201	0.001

Table 2. The results of the evaluation of LST

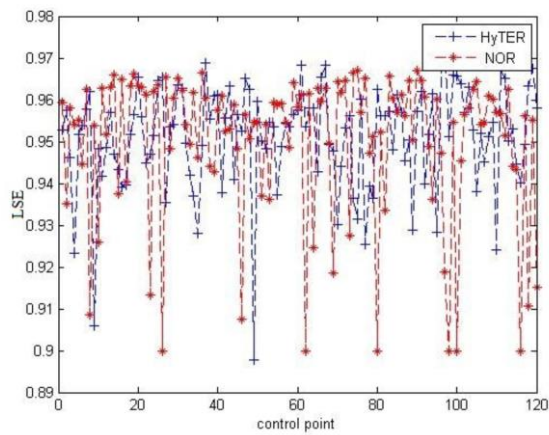
	REF		ALPHA		NOR		New Method	
	RMSE	SDE	RMSE	SDE	RMSE	SDE	RMSE	SDE
<b>LST</b>	1.41	0.296	2.06	0.587	1.84	0.372	1.6	0.298



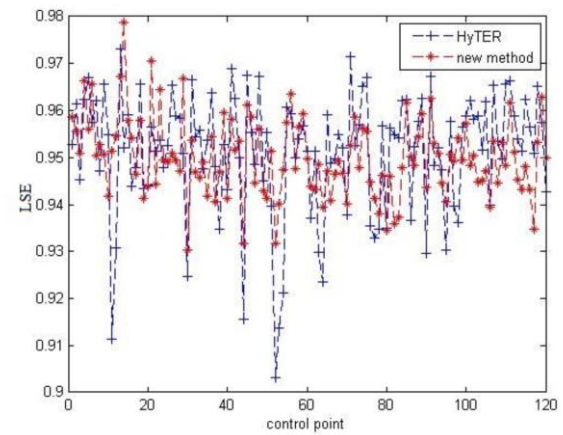
(a)



(b)



(c)



(d)

Figure 2. The obtained LSE values for 120 control points: (a) REF (b) ALPHA (c) NOR (d) New method

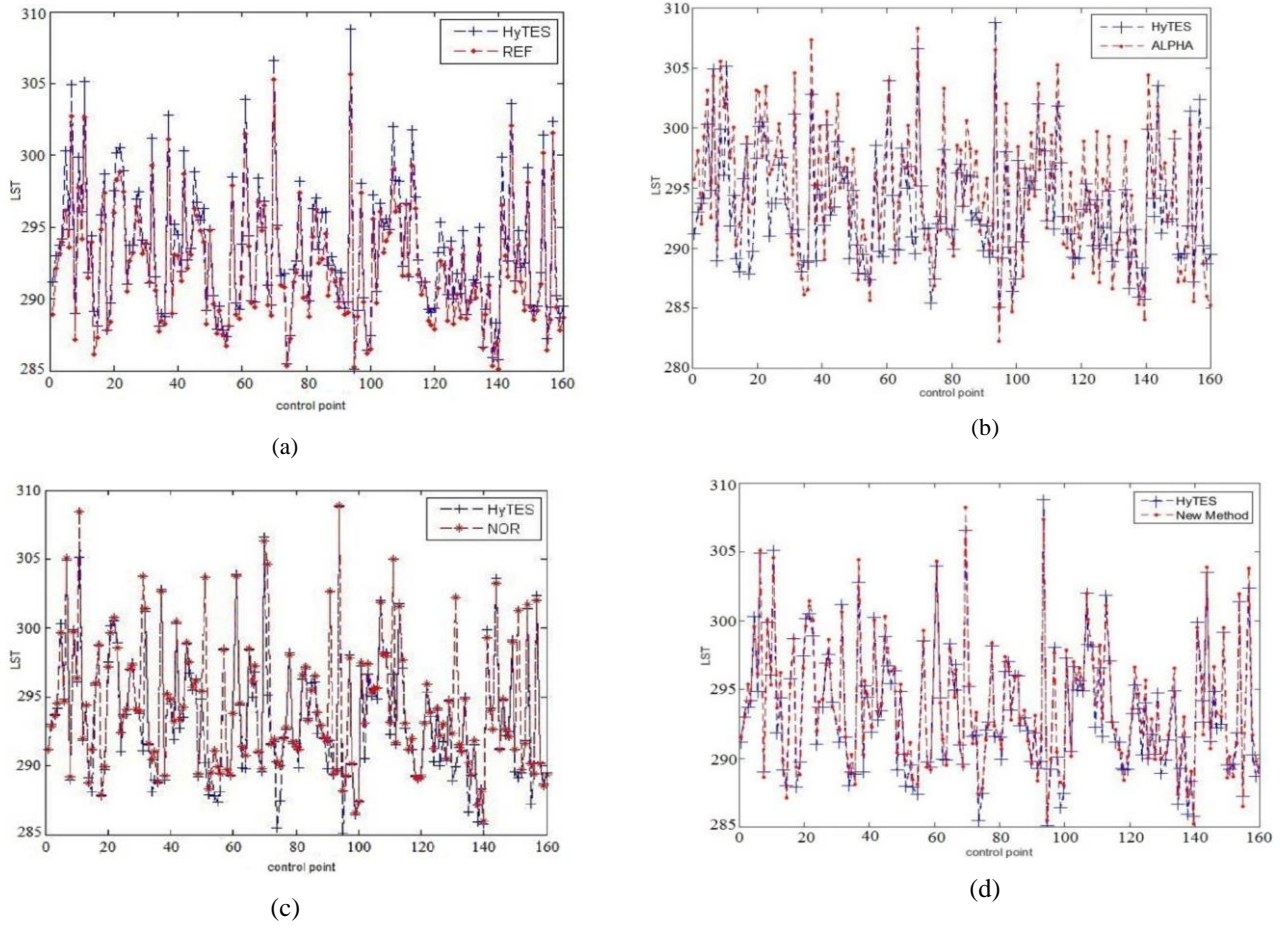


Figure 3. The obtained LST values for 160 control points: (a) REF (b) ALPHA (c) NOR (d) New method

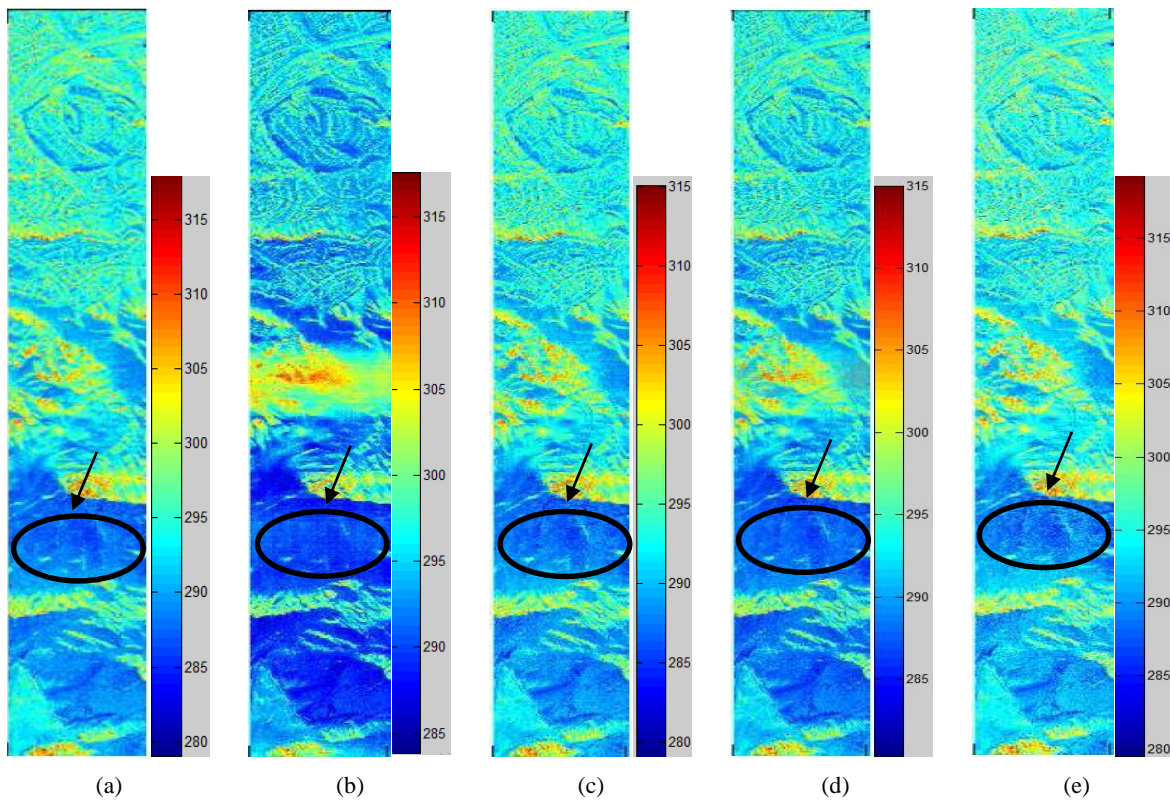


Figure 4. LST map: (a) HyTES (b) NOR (c) REF (d) New method (e) ALPHA

## 5. Conclusion

The HyTES sensors with 256 channels in the 7.5–12  $\mu\text{m}$  regions are needed to accurately retrieve the temperature and emissivity values. The scope of this study was to retrieve the land surface parameters and compare various methods to obtain the spectral emissivity and land surface temperature from the HyTES sensor. In this study, the land surface emissivity was obtained from four different methods: REF, Alpha, NOR and the new proposed method. In addition, the REF and NOR methods have been used for retrieval of the land surface temperature.

It can be observed that the REF method is simple in concept and application, but this method is only qualitative and some information will be lost in the reference channel. The atmospheric down-welling radiance is neglected in the Alpha emissivity method. The results show that the alpha method results are similar to other methods; therefore, the impact of the down-welling radiation is negligible. In the NOR method, the calculated temperature (Eq. (1)) is related to the blackbody surfaces so the final emissivity is also related only to the blackbody surfaces. Therefore, this method has a difficult application in vegetated areas. In order to solve this problem, the new method was proposed to smooth the calculated temperature (Eq. (1)). In the new proposed method, a constant emissivity ( $\epsilon_0 = 0.99$ ) was considered in all N channels for a given pixel, which enables N temperatures to be calculated for each pixel using Eq. (1) from their radiance. The calculated temperatures from Eq. (1) are related to the blackbody or near the blackbody surfaces. In NOR, the maximum value of N temperature for each pixel is considered as LST, so the obtained LST will only be exact for the areas with a blackbody surface. Therefore, the NOR method for other areas that are not blackbody acts as a blackbody surface, and the land surface emissivity that is obtained from this temperature is related to the blackbody surfaces and is higher than its real value. In order to improve the accuracy of the NOR method, the LST values that are obtained from Eq. (1) must be smoothed. For this purpose, the mean value of N temperatures was considered as LST, and was used to derive the emissivity for other channels using Eq. (2). Using this approach, the calculated temperature and emissivity values are not related only to the blackbody surfaces (Section 2).

Finally, the results of LST and LSEs derived from these algorithms were compared with the LST and LSE products of HyTES. The results in this study prove the feasibility of retrieving accurate estimates of the surface temperature and emissivity with HyTES data.

## References

- Aires, F., Chedin, A., Scott, N. A., & Rossow, W. B. (2002). A regularized neural net approach for retrieval of atmospheric and surface temperatures with the IASI instrument. *Journal of Applied Meteorology*, 41(2), 144-159.
- Bagavathiappan, S., Lahiri, B. B., Saravanan, T., Philip, J., & Jayakumar, T. (2013). Infrared thermography for condition monitoring—A review. *Infrared Physics & Technology*, 60, 35-55.
- Borel, C. C. (1998, July). Surface emissivity and temperature retrieval for a hyperspectral sensor. In *Geoscience and Remote Sensing Symposium Proceedings, 1998. IGARSS'98. 1998 IEEE International (Vol. 1, pp. 546-549)*. IEEE.
- Borel, C. C. (2003, March). ARTEMISS—an algorithm to retrieve temperature and emissivity from hyper-spectral thermal image data. In *28th Annual GOMACTech Conference, Hyperspectral Imaging Session (Vol. 31, pp. 1-4)*.
- Borel, C. (2008). Error analysis for a temperature and emissivity retrieval algorithm for hyperspectral imaging data. *International Journal of Remote Sensing*, 29(17-18), 5029-5045.
- Brandt, R., Bird, C., & Neuer, G. (2008). Emissivity reference paints for high temperature applications. *Measurement*, 41(7), 731-736.
- Chen, F., Yang, S., Su, Z., & Wang, K. (2016). Effect of emissivity uncertainty on surface temperature retrieval over urban areas: Investigations based on spectral libraries. *ISPRS journal of photogrammetry and remote sensing*, 114, 53-65.
- Dash, P., Göttsche, F. M., Olesen, F. S., & Fischer, H. (2002). Land surface temperature and emissivity estimation from passive sensor data: theory and practice—current trends. *International Journal of remote sensing*, 23(13), 2563-2594.
- Gillespie, A. R. (1985). Lithologic mapping of silicate rocks using TIMS. *The TIMS Data Users Workshop. JPL Publ*, 86-38.
- Gillespie, A., Rokugawa, S., Matsunaga, T., Cothorn, J. S., Hook, S., & Kahle, A. B. (1998). A temperature and emissivity separation algorithm for Advanced Spaceborne Thermal Emission and Reflection Radiometer (ASTER) images. *IEEE transactions on geoscience and remote sensing*, 36(4), 1113-1126.
- Gillespie, A. R., Rokugawa, S., Hook, S. J., Matsunaga, T., & Kahle, A. B. (1999). Temperature/emissivity separation algorithm theoretical basis document, version 2.4. ATBD contract NAS5-31372, NASA.
- Hu, T., Liu, Q., Du, Y., Li, H., Wang, H., & Cao, B. (2015). Analysis of the land surface temperature scaling problem: A case study of airborne and satellite data over the Heihe Basin. *Remote Sensing*, 7(5), 6489-6509.
- Jacob, F., Lesaignoux, A., Oliosio, A., Weiss, M., Caillault, K., Jacquemoud, S., ... & Lagouarde, J. P. (2017). Reassessment of the temperature-emissivity separation from multispectral thermal infrared data: Introducing the impact of vegetation canopy by simulating the cavity

- effect with the SAIL-Thermique model. *Remote Sensing of Environment*, 198, 160-172.
- Kahle, A. B., Madura, D. P., & Soha, J. M. (1980). Middle infrared multispectral aircraft scanner data: Analysis for geological applications. *Applied Optics*, 19(14), 2279-2290.
- Kealy, P. S. (1990). Estimation of emissivity and temperature using alpha coefficients. In *Proceedings of the Second Thermal Infrared Multispectral Scanner (TIMS) Workshop* (pp. 11-16).
- Kealy, P. S., & Hook, S. J. (1993). Separating temperature and emissivity in thermal infrared multispectral scanner data: Implications for recovering land surface temperatures. *IEEE Transactions on Geoscience and Remote Sensing*, 31(6), 1155-1164.
- Labbi, A., & Mokhnache, A. (2015). Derivation of split-window algorithm to retrieve land surface temperature from MSG-1 thermal infrared data. *European Journal of Remote Sensing*, 48(1), 719-742.
- Li, Z. L., Becker, F., Stoll, M. P., & Wan, Z. (1999). Evaluation of six methods for extracting relative emissivity spectra from thermal infrared images. *Remote sensing of Environment*, 69(3), 197-214.
- Li, Z. L., Wu, H., Wang, N., Qiu, S., Sobrino, J. A., Wan, Z., ... & Yan, G. (2013). Land surface emissivity retrieval from satellite data. *International Journal of Remote Sensing*, 34(9-10), 3084-3127.
- Marinetti, S., & Cesaratto, P. G. (2012). Emissivity estimation for accurate quantitative thermography. *NDT & E International*, 51, 127-134.
- Nunak, T., Rakrueangdet, K., Nunak, N., & Suesut, T. (2015, March). Thermal image resolution on angular emissivity measurements using infrared thermography. In *Proceedings of the International MultiConference of Engineers and Computer Scientists (Vol. 1, pp. 18-20)*.
- Ultra-Carrió, R., Cubero-Castan, M., Briottet, X., & Sobrino, J. A. (2014). Analysis of the performance of the TES algorithm over urban areas. *IEEE Transactions on Geoscience and Remote Sensing*, 52(11), 6989-6998.
- Peres, L. F., & DaCamara, C. C. (2005). Emissivity maps to retrieve land-surface temperature from MSG/SEVIRI. *IEEE Transactions on Geoscience and Remote Sensing*, 43(8), 1834-1844.
- Rivera, G. (2012). *Hyperspectral Thermal Emission Spectrometer*. <https://hytes.jpl.nasa.gov/>.
- Rozenstein, O., Qin, Z., Derimian, Y., & Karnieli, A. (2014). Derivation of land surface temperature for Landsat-8 TIRS using a split window algorithm. *Sensors*, 14(4), 5768-5780.
- Singh, D., & Bhatia, R. C. (2007). Retrieval of atmospheric temperature and moisture profiles from satellite data over India using the ICI inversion model.
- Sobrino, J. A., & Raissouni, N. (2000). Toward remote sensing methods for land cover dynamic monitoring: application to Morocco. *International journal of remote sensing*, 21(2), 353-366.
- Sobrino, J. A., Raissouni, N., & Li, Z. L. (2001). A comparative study of land surface emissivity retrieval from NOAA data. *Remote Sensing of Environment*, 75(2), 256-266.
- Sobrino, J. A., Jiménez-Muñoz, J. C., & Verhoef, W. (2005). Canopy directional emissivity: Comparison between models. *Remote Sensing of Environment*, 99(3), 304-314.
- Sobrino, J. A., Jiménez-Muñoz, J. C., Zarco-Tejada, P. J., Sepulcre-Cantó, G., & de Miguel, E. (2006). Land surface temperature derived from airborne hyperspectral scanner thermal infrared data. *Remote Sensing of Environment*, 102(1-2), 99-115.
- Sun, D., & Pinker, R. T. (2003). Estimation of land surface temperature from a Geostationary Operational Environmental Satellite (GOES- 8). *Journal of geophysical research: atmospheres*, 108(D11).
- Tang, H., & Li, Z. L. (2013). *Quantitative Remote Sensing in Thermal Infrared: Theory and Applications*. Springer Science & Business Media.
- Valor, E., & Caselles, V. (1996). Mapping land surface emissivity from NDVI: Application to European, African, and South American areas. *Remote sensing of Environment*, 57(3), 167-184.
- Wang, N., Tang, B. H., Li, C., & Li, Z. L. (2010, July). A generalized neural network for simultaneous retrieval of atmospheric profiles and surface temperature from hyperspectral thermal infrared data. In *Geoscience and Remote Sensing Symposium (IGARSS), 2010 IEEE International*, 1055-1058.
- Wang, N., Wu, H., Nerry, F., Li, C., & Li, Z. L. (2011). Temperature and emissivity retrievals from hyperspectral thermal infrared data using linear spectral emissivity constraint. *IEEE Transactions on Geoscience and Remote Sensing*, 49(4), 1291-1303.
- Wang, N., Li, Z. L., Tang, B. H., Zeng, F., & Li, C. (2013). Retrieval of atmospheric and land surface parameters from satellite-based thermal infrared hyperspectral data using a neural network technique. *International Journal of Remote Sensing*, 34(9-10), 3485-3502.
- Young, S. J., Johnson, B. R., & Hackwell, J. A. (2002). An in-scene method for atmospheric compensation of thermal hyperspectral data. *Journal of Geophysical Research: Atmospheres*, 107(D24).
- Zhao, E., Qian, Y., Gao, C., Huo, H., Jiang, X., & Kong, X. (2014). Land surface temperature retrieval using airborne hyperspectral scanner daytime mid-infrared data. *Remote Sensing*, 6(12), 12667-12685.
- Zhong, X., Huo, X., Ren, C., Labed, J., & Li, Z. L. (2016). Retrieving land surface temperature from hyperspectral thermal infrared data using a multi-channel method. *Sensors*, 16(5), 687.